Electronic Supplementary Material (ESI) for Nanoscale.

Supporting information for

Iodide-doped Precious Metal Nanoparticles: Measuring Oxidative Stress *in vivo* via Photoacoustic Imaging

Yash Mantri [1], Barak Davidi [2], Jeanne E. Lemaster [3], Ali Hariri [3] and Jesse V. Jokerst* [3,4,5]

[1] Department of Bioengineering University of California, San Diego, La Jolla, CA, USA.,

[2] Department of Physics, Fairfield University, Fairfield, CT, USA.

[3] Department of NanoEngineering, University of California, San Diego, La Jolla, CA, USA.

[4] Materials Science Program, University of California, San Diego, La Jolla, CA, USA.

[5] Department of Radiology, University of California, San Diego, La Jolla, CA, USA.

*Corresponding Author

E-mail: jjokerst@ucsd.edu

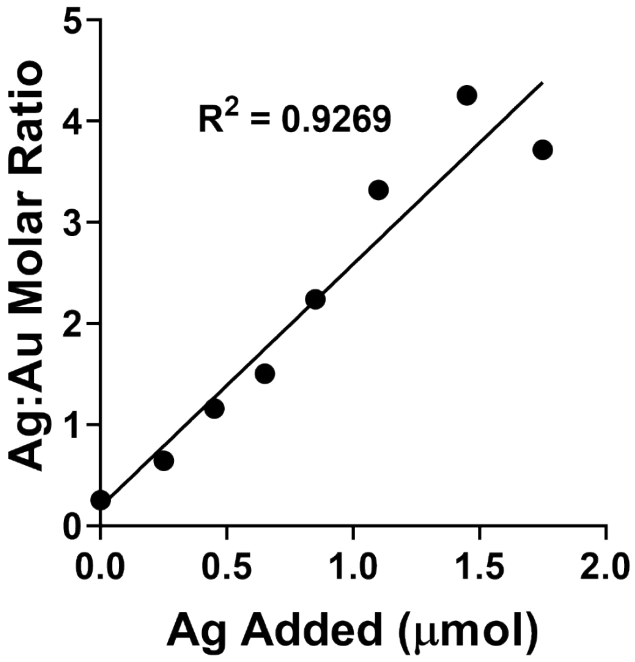

Figure S1. Final immobilized Ag:Au molar ratio measured by ICP-MS. Ag shell thickness can be controlled by adding increasing amounts of $AgNO_3$ during the Ag coating step.

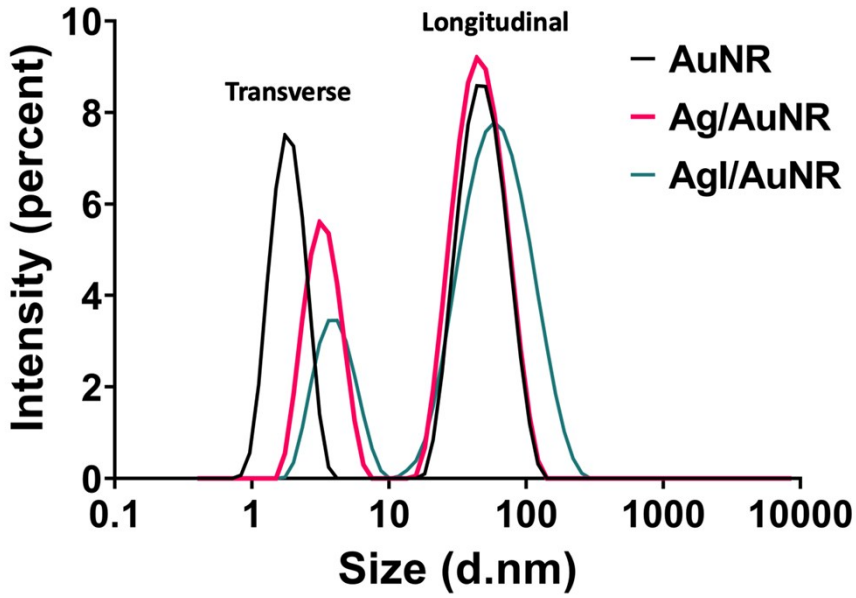

Figure S2. Nanoparticles characterized using dynamic light scattering (DLS). Two peaks can be observed for the transverse and longitudinal sections of the rod structure. Silver deposition is more favorable on the {110} facet of the gold which is along the longitudinal edge. As a result, the rod becomes thicker, but the length remains relatively the same. Doping with Iodide results in a 1 nm increase in shell thickness which can be attributed to AgI_3O_8 complex formation. The poly dispersity index (PDI) for AuNR: 0.55, Ag/AuNR: 0.59 and AgI/AuNR: 0.67. The PDI is unusually high because DLS assumes the particles are spherical and is not optimized to characterize rod like structures.

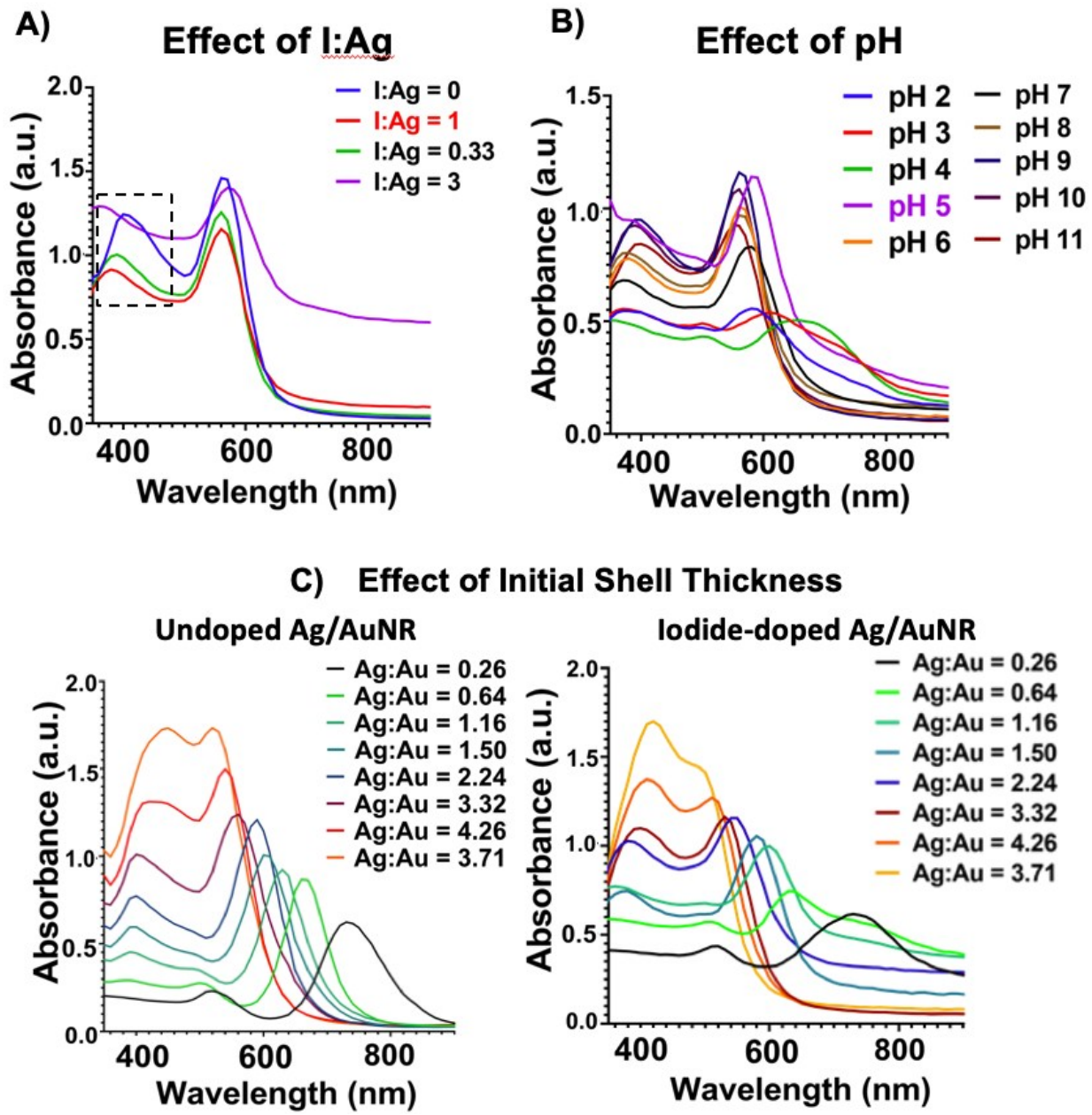

Figure S3. Optimizing reaction conditions for iodide doping. Effect of I:Ag molar ratio (**A**). An I:Ag greater than 1 results in particle destabilization whereas <1 does not maximize doping. A 1:1 ratio is optimal. Effect of pH on doping (**B**). Iodide can be doped into Ag under acidic conditions but highly acidic conditions result in Ag shell etching; pH 5 was optimal. Effect of initial Ag shell thickness on doping efficiency (**C**). A thin shell is more susceptible to damage under acidic conditions than a thick shell (Ag:Au molar ratio > 3.32). Hence, A Ag:Au molar ratio > 3.32 is found to be optimal for shell doping.

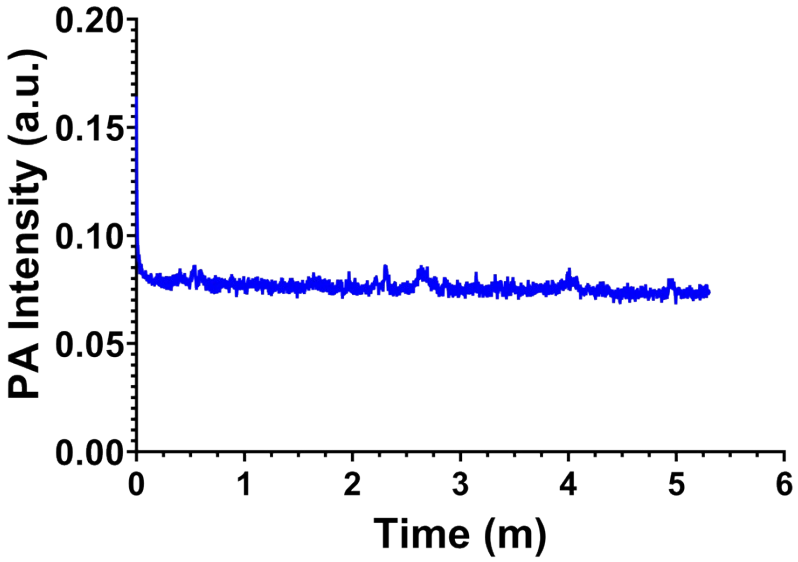

Figure S4. Photostability. Synthesized AgI/AuNRs show a 17% decrease in PA amplitude over 5 minutes of 680 nm illumination. PA intensity is low here because AgI/AuNRs have peak absorbance at 578 nm.

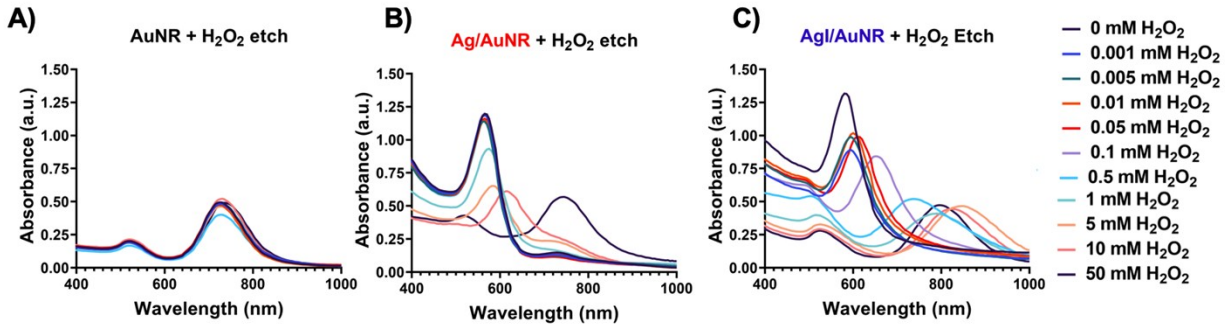

Figure S5. H_2O_2 etching. AuNR is unaffected when treated with varying concentrations of H_2O_2 (**A**). Ag/AuNR starts to etch at 10 mM (**B**) and AgI/AuNR starts to etch at 0.05 mM H_2O_2 (**C**).

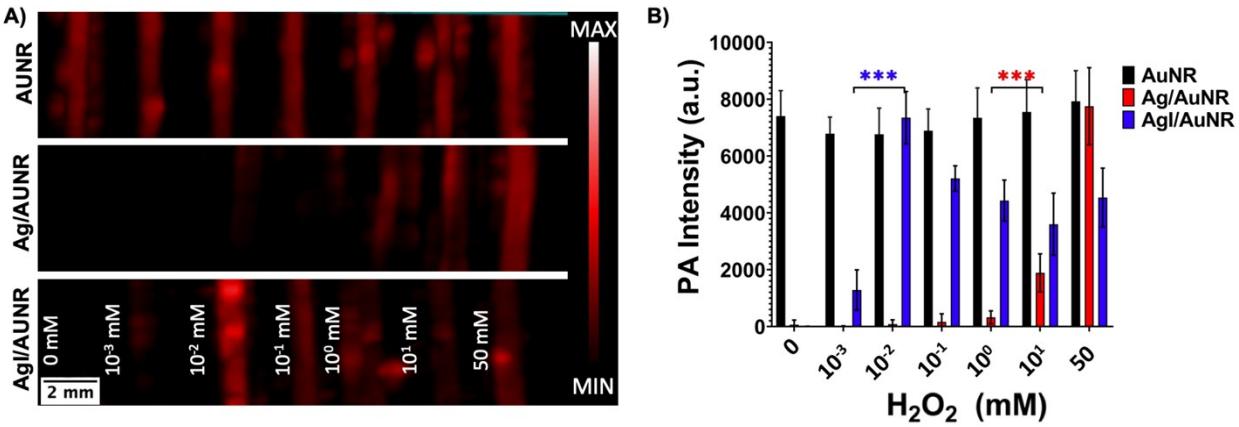

Figure S6. Photoacoustic imaging of H_2O_2 etching. Photoacoustic images of AuNR, Ag/AuNR, and AgI/AuNR treated with varying concentrations of H_2O_2 (**A**). Plot comparing photoacoustic intensity after treatment with varying concentrations of H_2O_2 (**B**). There is a significant ($p < 0.001$) increase in photoacoustic intensity at 10^{-2} mM H_2O_2 for AgI/AuNR and at 10 mM for Ag/AuNR. AgI/AuNR is 1000-fold more sensitive to H_2O_2 than undoped Ag/AuNR. The error bars represent the standard deviation of six regions-of-interest.

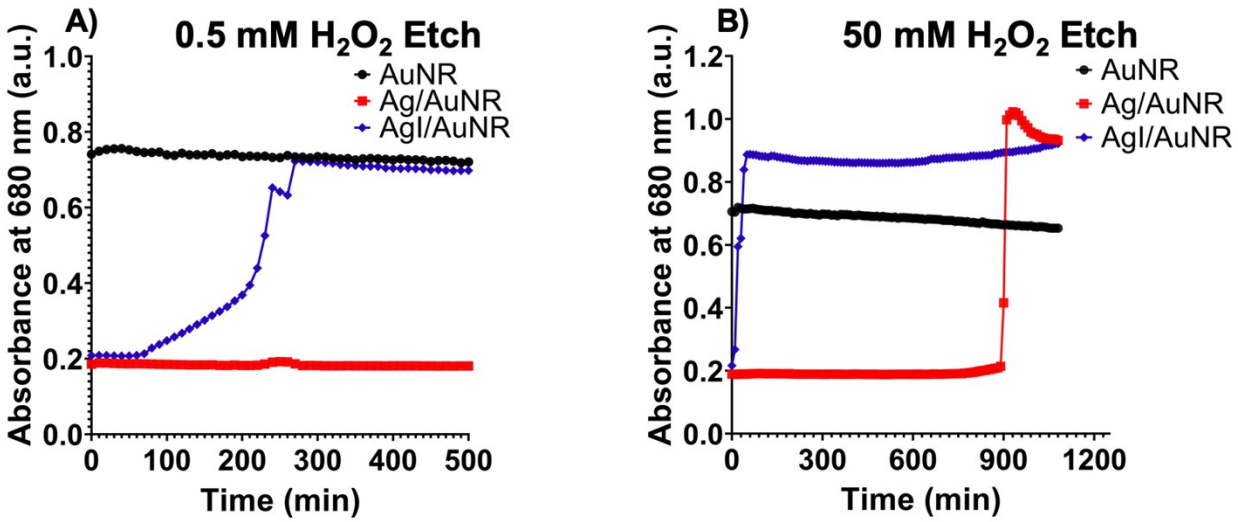

Figure S7. H_2O_2 etching kinetics. At 0.5 mM H_2O_2 AgI/AuNR takes ~5 hours to completely etch whereas AuNR and Ag/AuNR show no change in absorbance at 680 nm (**A**). At 50 mM AgI/AuNR etches 45 times faster than undoped particles which take over 15 hours to etch (**B**).

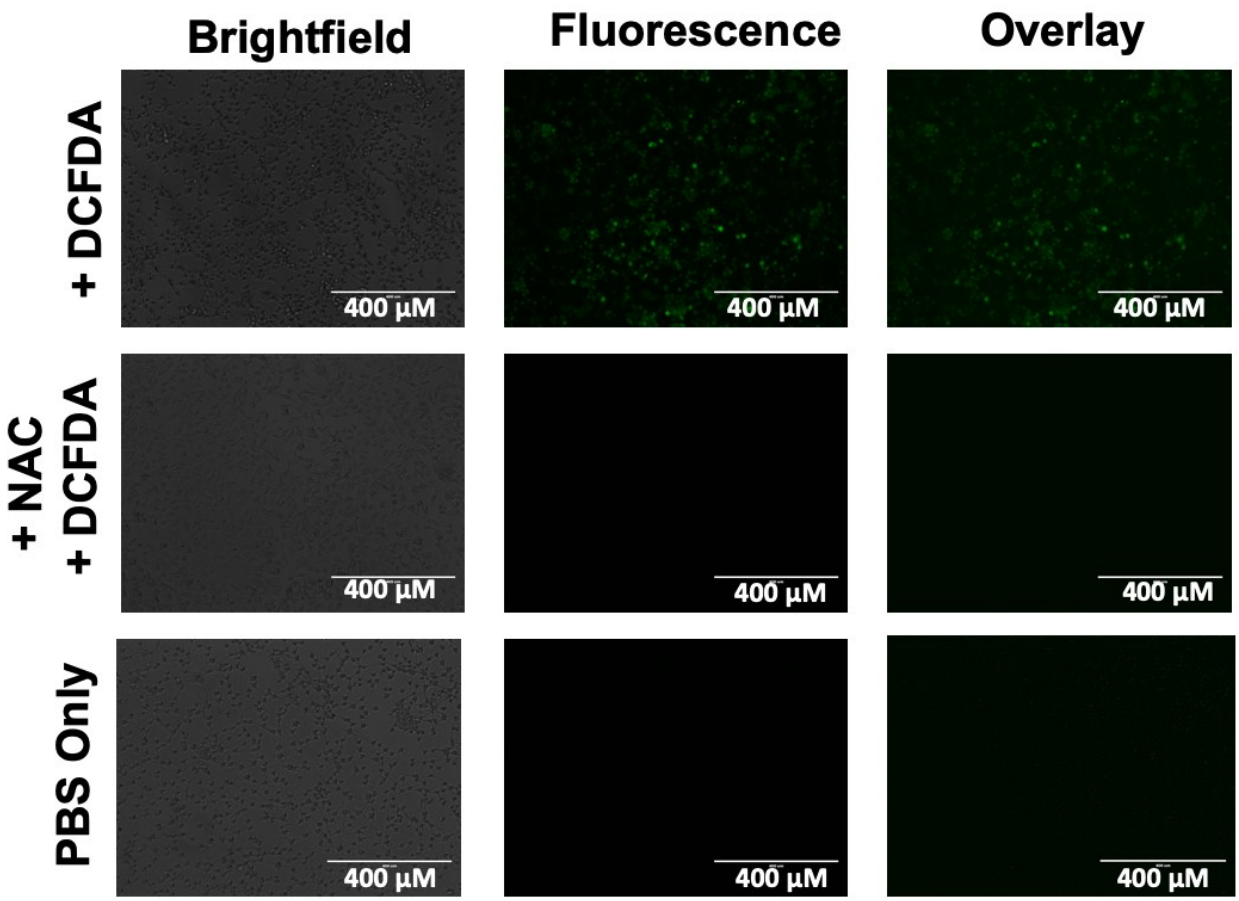

Figure S8. SKOV3 DCFDA assay. Ovarian cancer (SKOV3) cells naturally produce RONS that can be scavenged with NAC. DCFDA is a ROS-sensitive fluorophore that is emissive only in the presence of ROS. Cells treated with DCFDA showed green fluorescence whereas cells treated with DCFDA + NAC showed no fluorescence.

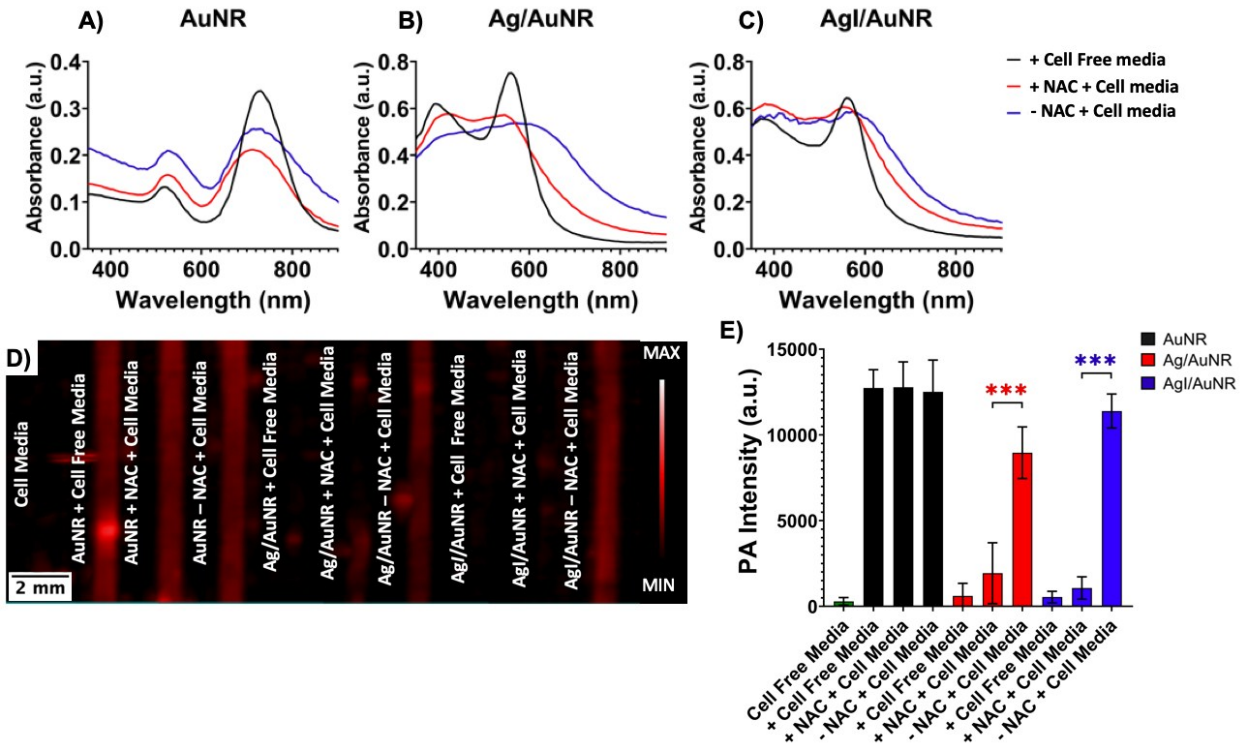

Figure S9. SKOV3-generated RONS photoacoustic response. Absorbance spectra of AuNR, Ag/AuNR and AgI/AuNR when treated with cell free media, + NAC + cell media and – NAC + cell media. NAC is a RONS scavenger. Absorbance at 680 nm increases more when treated with – NAC + cell media (**A-C**). Photoacoustic image at 680 nm of samples from A-C (**D**). Cell-free media has negligible photoacoustic signal. AuNR shows no change in signal with or without RONS scavenging. Ag/AuNR and AgI/AuNR both show etching when treated with – NAC + cell media (RONS enriched) that leads to increased PA signal (**E**). ($p < 0.001$) Error bars represent standard deviation of six regions-of-interest

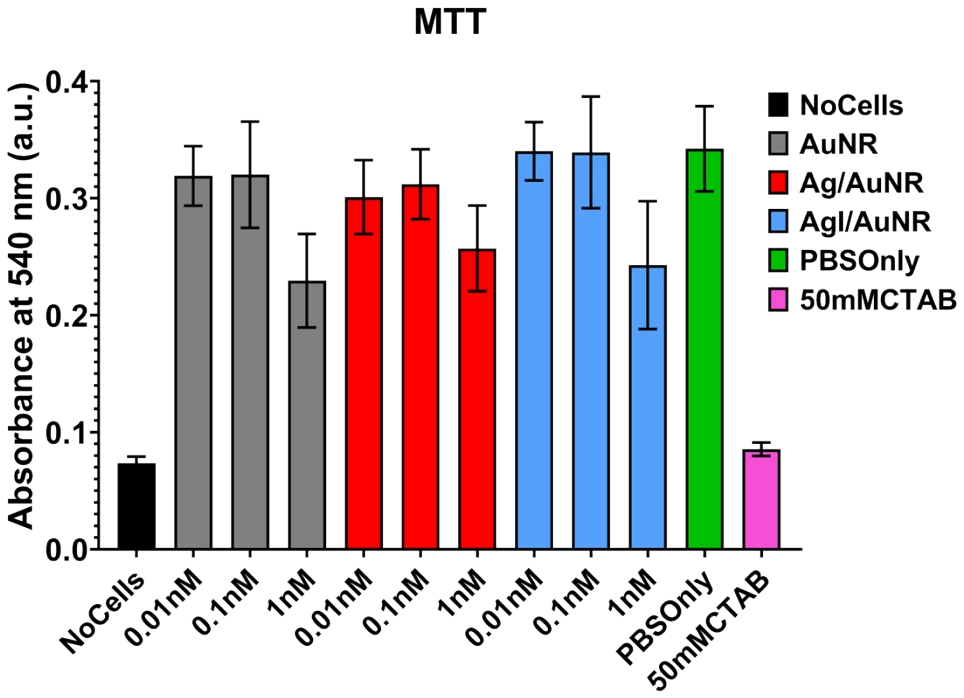

Figure S10. Cell cytotoxicity assay. At lower concentrations of 0.01 nM and 0.1nM, synthesized particles are not significantly more toxic than PBS only negative control. At higher concentrations of 1 nM, particles exhibit higher toxicity due to higher amounts of residual CTAB. All *in vivo* experiments were performed at 0.3 nM particle concentration.

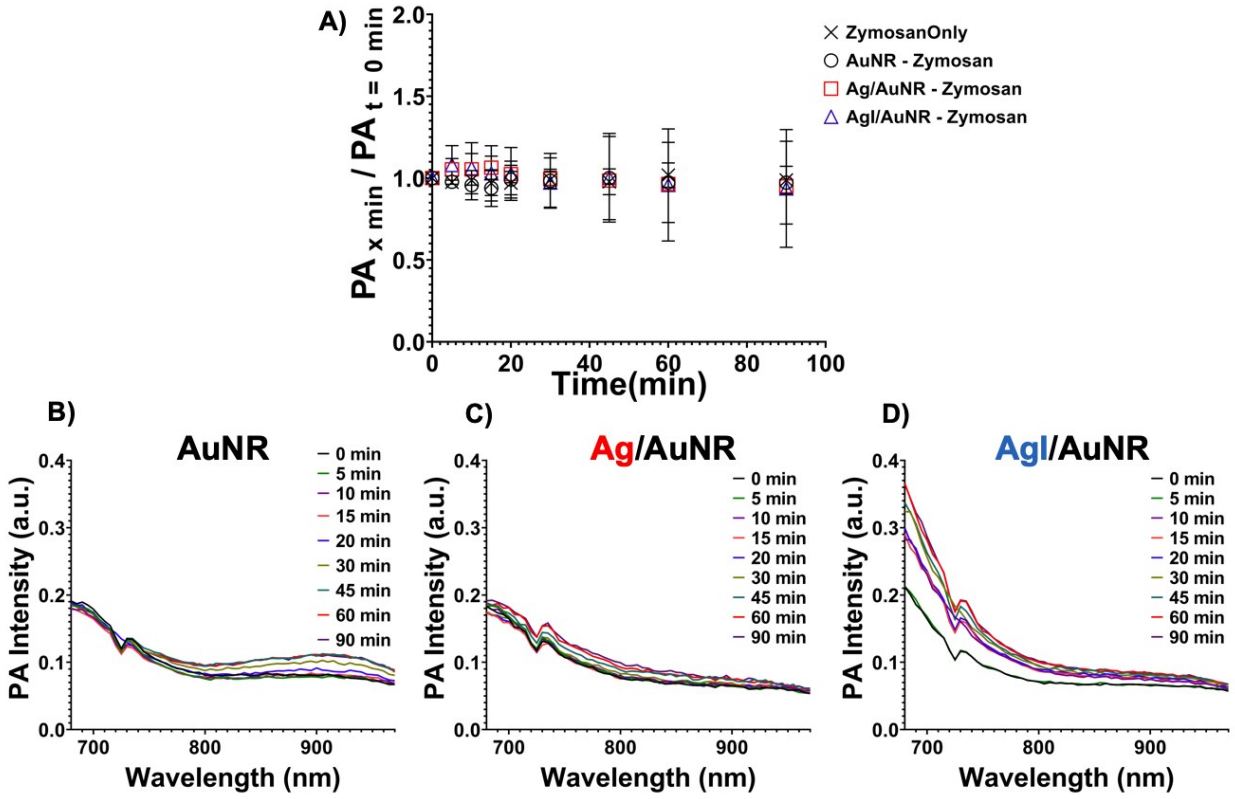

Figure S11. ***In vivo*** **RONS sensing.** Photoacoustic intensity at t = x min / photoacoustic intensity at t = 0 min for zymosan only and nanoparticles in the absence of zymosan (**A**). There is no RONS generation without Zymosan as a result the particles show no change in photoacoustic intensity compared to their baseline at t= 0 min. Photoacoustic spectra of AuNR, Ag/AuNR, and AgI/AuNR over 90 minutes in the presence of zymosan (**B-D**). AuNR and Ag/AuNR show no change in spectra over 90 min whereas AgI/AuNR shows a clear increase in signal at 680 nm.